

Copyright is owned by the Author of the thesis. Permission is given for a copy to be downloaded by an individual for the purpose of research and private study only. The thesis may not be reproduced elsewhere without the permission of the Author.

Electromagnetic propagation through non-dissipative and dissipative barriers

A thesis presented in partial fulfillment of
the requirements for the degree of
Master of Science
in Physics at
Massey University
Palmerston North, New Zealand

by

Avi Shalav

May 2002

Acknowledgments

There are a number of people whom without their support, this thesis would not have been made possible. Firstly, I would like to thank Neil Pinder my supervisor who has taught me understanding, confidence and ingenuity I had not previously known possible.

Secondly, I would also like to thank my family for their continual love and encouragement.

And finally, I would like to thank my friends and work colleagues who have taught me that persistence does pay off and that 'giving up' is never an option.

Abstract

A Matlab simulation was developed to help visualise and investigate electromagnetic tunnelling through particular non-dissipative and dissipative barriers within a waveguide. The theory behind the simulation is based on a transmission line model that accurately predicts experimental results and is shown to be equivalent to previous numerical and quantum tunnelling models.

A few useful speeds referring to electromagnetic waves have been defined and utilised to calculate the speeds at which different incident time signals penetrate electromagnetic barriers.

Due to bandwidth restrictions, the created incident time signals had wavepacket properties. The importance of resampling an oscillating signal at the appropriate frequency to avoid aliasing has been recognised.

The definition and creation of matched signals that can penetrate long barriers yet remain a single pulse have been investigated. Such signals will have no practical application since the attenuation will deem the transmitted signals immeasurable. However, the speeds through these larger barrier lengths will have a smaller uncertainty since the time delays are longer. Most of the signal distortion depends only on the barrier interfaces rather than the barrier length.

Penetration through dissipative barriers gives speeds below the vacuum speed of light for all barrier lengths investigated. Faster than light speeds are however predicted for penetration through non-dissipative barriers greater than about 4cm.

Contents

Acknowledgements	i
Abstract.....	ii
Contents.....	iii
List of figures.....	vii

Chapter 1

Introduction	1
1.1 Tunnelling and the collapse of causality	1
1.2 The analogy between quantum and electromagnetic tunnelling	2
1.3 Tunnelling time and the Hartman effect	4
1.4 Electromagnetic tunnelling through a waveguide.....	5

Chapter 2

Non-dissipative and dissipative electromagnetic barriers within a waveguide	6
2.1 Electromagnetic properties within a waveguide	6
2.1.1 Introduction to the waveguide.....	6
2.1.2 Field configurations within a waveguide	8
2.2 Waveguide properties with a potential barrier	9
2.2.1 Design of a waveguide with a potential barrier.....	9
2.2.2 Penetration through non-dissipative and dissipative waveguide barriers.....	10
2.2.3 The Frequency Constraints.....	12
2.2.4 Electromagnetic properties of a non-dissipative barrier.....	14
2.2.5 Electromagnetic properties of a dissipative barrier	14
2.3 Numerical and analytical models for the transmission coefficient through non-dissipative and dissipative barriers.....	15
2.3.1 A Quantum model	15
2.3.2 Previous waveguide models	16
2.3.3 A transmission line model.....	18
2.3.4 Model similarities.....	19
2.4 Speeds of Light	19

2.4.1	Phase and Group speeds.....	20
2.4.2	The Energy Speed.....	22
2.4.2.1	Energy speed through non-dissipative barriers	22
2.4.2.2	Energy speed through dissipative barriers.....	24
2.4.3	Signal speed.....	25
2.4.4	The correlation speed.....	25

Chapter 3

A theoretical study of non-dissipative and dissipative barrier penetration within a waveguide.....

3.1	Creating an incident signal.....	27
3.1.1	The Discrete Fourier Transform (DFT)	27
3.1.2	Time-sampling of a wave-packet signal	30
3.2	Incident time signal construction	30
3.3	Non-dissipative barrier penetration using the transmission line model.....	37
3.3.1	Attenuation and phase as a function of frequency	37
3.3.2	The Transmitted Amplitude Spectrum.....	40
3.3.3	Attenuation and phase as a function of time	42
3.3.4	The Transmitted Time Signal	45
3.3.4.1	Wavepacket peak time differences.....	45
3.3.4.2	Sampling the envelope of the transmitted time signal.....	47
3.3.5	Speeds through a non-dissipative barrier	49
3.4	Dissipative barrier penetration using the transmission line model	55
3.4.1	Attenuation and phase as a function of frequency	55
3.4.2	The Transmitted amplitude spectrum	58
3.4.3	Attenuation and phase as a function of time	59
3.4.4	The transmitted time signal.....	59
3.4.4.1	Wavepacket peak time differences.....	59
3.4.4.2	Sampling the envelope of the transmitted time signal.....	60
3.4.5	Speeds through a dissipative barrier	61

Chapter 4	
Creation of matched incident signals able to penetrate long non-dissipative barriers	66
4.1	Piecewise linear Model for the attenuation as a function of frequency through a non-dissipative barrier
	67
4.2	A matched Gaussian signal
	70
4.2.1	Creating a matched Gaussian shaped amplitude spectrum.....
	70
4.2.2	The matched Gaussian transmitted time signal and its associated amplitude spectrum
	72
4.2.3	Speeds of the matched Gaussian signal.....
	74
4.3	An improved matched signal
	76
4.3.1	Creating a improved matched amplitude spectrum.....
	77
4.3.2	The improved matched transmitted time signal and its associated amplitude spectrum
	77
4.3.3	Speeds of the improved matched signal.....
	79
4.4	Verification of the attenuation model
	81
4.5	Gaussian and Shalav amplitude spectrum curves
	82
Chapter 5	
Conclusion	84
5.1	Overview
	84
5.1.1	Non-dissipative barrier penetration.....
	84
5.1.2	Dissipative barrier penetration
	85
5.1.3	Matched Signals penetrating non-dissipative barriers
	85
5.2	Signal Limitations and improvements
	85
5.2.1	Bandwidth constraints and wavepackets.....
	85
5.2.2	Matched signal limitations.....
	86
5.3	Is causality violated?
	86
5.3.1	A practical approach to causality
	87
5.3.2	A theoretical approach to causality.....
	87
5.4	Future developments
	88
5.4.1	Further investigations
	88
5.4.1.1	Utilising the Matlab EBP simulation.....
	88
5.4.1.2	Other matched signals
	88

5.4.2	Applications	89
Appendices	90
Appendix A	Selected mathematical calculations and proofs	90
Appendix B	Selected transmitted time signal envelopes after penetrating a non-dissipative barrier	94
Appendix C	Amplitude spectra for selected signal shapes at different non- dissipative barrier lengths	101
Appendix D	Construction of a Shalav curve	108
Appendix E	Matlab Electromagnetic Barrier Penetration (EBP) simulation user guide	111

List of Figures

Figure 1.1: Tunnelling analogies.....	3
Figure 1.2: Experimental results.....	5
Figure 2.1: A hollow rectangular metallic waveguide.	7
Figure 2.2: Field components of the dominant mode.....	8
Figure 2.3: Field Configurations for the dominant mode inside a hollow rectangular waveguide.....	9
Figure 2.4: A Waveguide with a barrier of length ℓ	10
Figure 2.5: Brillouin Diagram for the propagation in a rectangular dielectric filled waveguide.....	13
Figure 2.6: Brillouin Diagram comparing dominant mode frequency bands through a waveguide with a non-dissipative barrier.....	13
Figure 3.1: The time domain wave-packet reconstruction of a Gaussian signal.....	29
Figure 3.2: A periodic Gaussian signal created from the DFT.....	31
Figure 3.3: The required signal shape to be created using the DFT	32
Figure 3.4: Amplitude spectra for a log-Gaussian incident signal	33
Figure 3.5: The created and time-sampled (envelope) signals of $x(t)$ required for a non-dissipative analysis.	34
Figure 3.6: Change in apparent period..	35
Figure 3.7: Re-constructed envelopes of log-Gaussian time signals.....	36
Figure 3.8: $ T ^2$ against frequency for penetration through a non-dissipative barrier.....	38
Figure 3.9: Phase against frequency for penetration through a non-dissipative barrier....	38
Figure 3.10: Phase against frequency for penetration through a short (<2cm) non-dissipative barrier	39
Figure 3.11: Phase against frequency for penetration through a long (>2cm) non-dissipative barrier	40
Figure 3.12: The transmitted normalised amplitude spectrum for an incident Gaussian signal traversing a non-dissipative barrier.....	42

Figure 3.13: Graph showing the linearity between the average intensity and barrier length for non-dissipative barriers.....	43
Figure 3.14: Phase shift for a few selected frequencies..	44
Figure 3.15: Time differences between adjacent peaks for a Gaussian wavepacket after penetrating different non-dissipative barrier lengths.	46
Figure 3.16: The incident and transmitted time signal for a Gaussian shaped wavepacket.....	47
Figure 3.17: The normalised transmitted time signal envelopes for a Gaussian shaped incident signal penetrating various barrier lengths..	48
Figure 3.18: Phase speed through the waveguide as a function of frequency.....	50
Figure 3.19: Group speeds through the waveguide as a function of frequency..	50
Figure 3.20: Hartman phase speed as a function of frequency for non-dissipative barriers.....	51
Figure 3.21: Hartman group speed as a function of frequency.	51
Figure 3.22: Padded incident and transmitted time envelopes used to find the cross-correlation speed.	53
Figure 3.23: Auto and cross-correlation curves.	53
Figure 3.24: Speed as a function of barrier length for a Gaussian shaped time signal penetrating a non-dissipative barrier.....	54
Figure 3.25: $ T ^2$ against frequency for penetration through a dissipative barrier	57
Figure 3.26: Phase against frequency for penetration through a non-dissipative barrier.....	57
Figure 3.27: The normalized transmitted amplitude spectra of a Gaussian signal penetrating a dissipative barrier.	58
Figure 3.28: Time differences between adjacent peaks for a Gaussian wavepacket after penetrating different dissipative barrier lengths.	60
Figure 3.29: The normalised transmitted time signal envelopes for a Gaussian shaped incident signal penetrating various dissipative barrier lengths.....	61
Figure 3.30: Magnitudes of the phase speeds through a dissipative barrier within a waveguide..	63
Figure 3.31: Magnitudes of the Group speeds through a dissipative barrier	

within a waveguide.....	63
Figure 3.32: Hartman phase speeds as a function of frequency.....	64
Figure 3.33: Hartman Group speeds as a function of frequency.....	64
Figure 3.34: Speed as a function of barrier length for a Gaussian shaped signal penetrating a dissipative barrier.....	65
Figure 4.1: Curves showing the attenuation as a function of frequency for increasing non-dissipative barrier lengths.	67
Figure 4.2: Regions of interest of a $\ln(T)$ against $\ln(f)$ graph.	68
Figure 4.3: Creation of a matched Gaussian amplitude spectrum.....	71
Figure 4.4: Transmitted envelope of a matched Gaussian incident signal through barriers up to 150cm.....	72
Figure 4.5: The transmitted amplitude spectra of a matched Gaussian time signal.....	73
Figure 4.6: Migration of the peak of the amplitude spectrum with barrier length.	74
Figure 4.7: Graph showing the linearity of the average Hartman group speed and signal speed (fraction=1) for increasing barrier lengths.....	75
Figure 4.8: A Gaussian curve and a similar shaped Shalav curve.....	76
Figure 4.9: Transmitted envelope of an improved matched incident signal through barriers up to 300cm.....	78
Figure 4.10: The transmitted amplitude spectra of a Shalav amplitude spectrum..	78
Figure 4.11: Migration of the peak of the amplitude spectrum with barrier length for matched Shalav curves.....	79
Figure 4.12: Average Hartman group speed and signal speed (fraction=1) for increasing barrier lengths for an improved matched signal.....	80
Figure 4.13: Effect on curve shapes when the barrier length is increased..	81
Figure 4.14: Graph showing at which frequency Gaussian shaped amplitude spectrum peaks for different barrier lengths..	82
Figure 4.15: Graph showing at which frequency Shalav shaped amplitude spectrum peaks for different barrier lengths.	83
Figure D1.1: Shalav curve created from simple Matlab instructions.....	110

Chapter 1

Introduction

1.1 *Tunnelling and the collapse of causality*

Causality allows two different observers to agree on a cause and an effect of a particular event and is a fundamental assumption of modern relativistic physics.

According to Einstein's theory of special relativity, if a signal could travel faster than the speed of light then there would be a violation of causality. Signals would seem to arrive before they departed and they could even appear to travel backwards in time. By making use of superluminal signals it would be possible to communicate with the past, which is not logically possible. To overcome this 'logical disaster' it has been assumed throughout the physics world that no signal may travel faster than c , the speed of light in free space [1]. Speeds greater than c , are defined to be superluminal while speeds less than c are defined to be subluminal.

In recent years, experiments on quantum barrier tunnelling and electromagnetic barrier tunnelling have yielded superluminal speeds creating wide public interest [2, 3]. Experiments in the quantum regime consist of two-photon interferometry [4], or tachyonlike excitations in inverted two level media [5, 6]. Experiments in the electromagnetic regime consist of microwave propagation over short distances using launcher and receiver horns [7], microwave transmission through undersized waveguides [8-11], photonic waveguide/heterostructure tunnelling experiments [12, 13] and more recently total internal reflection in a double prism experiment [14]. Electromagnetic barriers can magnify the time scale up to nanoseconds so microwave experiments can be

compared with theoretical predictions taken from quantum tunnelling which require a less accessible time range [15]. This is because the length of the barrier must be of the order of the wavelength of the radiation for measurable tunnelling to occur. Propagation times in the nanosecond regime can be obtained with microwave barriers (electromagnetic radiation with cm wavelengths).

1.2 The analogy between quantum and electromagnetic tunnelling

The analogy between quantum tunnelling and electromagnetic (or photon) tunnelling is well known [16-18]. The analogy is from a similarity between the two fundamental equations governing these seemingly different tunnelling situations. The one dimensional Schrödinger wave equation is the basic relationship for determining wave functions and energy levels of a quantum particle. The time independent Schrödinger equation can be written as

$$\nabla^2\psi + \frac{2m}{\hbar^2}(E - U)\psi = 0 \quad (1.1)$$

Where ψ is the wavefunction, m is the particle mass, \hbar is Planck's constant divided by 2π , E is the particle energy, and U is the uniform potential energy.

The wave equation derived from Maxwell's equations for classical electromagnetic fields is

$$\nabla^2 E = \mu\sigma \frac{\partial E}{\partial t} + \mu\epsilon \frac{\partial^2 E}{\partial t^2} \quad (1.2)$$

Where μ is the coefficient of permeability of the medium (usually equal to that of free space μ_0), ϵ is the coefficient of permittivity of the medium, σ is the conductivity of the medium and in this case, E is the electromagnetic wave function usually a sinusoid of the form $e^{i\omega t - \gamma z}$ where ω is the angular frequency, γ is the complex propagation constant and z is the direction of propagation. If there were no losses ($\sigma = 0$) then

$$\nabla^2 E = \mu\epsilon \frac{\partial^2 E}{\partial t^2} \quad (1.3)$$

Doing the differentiation

$$\frac{\partial^2 E}{\partial t^2} = -\omega^2 E \quad (1.4)$$

and substituting in

$$\mu\epsilon = \frac{n^2}{c^2} \quad (1.5)$$

Where n is the refractive index of the medium and c is the speed of light in a vacuum, Equation (1.3) can be re-written as:

$$\nabla^2 E + \frac{n^2 \omega^2}{c^2} E = 0 \quad (1.6)$$

Equations (1.1) and (1.6) are formally identical and if we write:

$$\frac{n^2 \omega^2}{c^2} = \frac{2m}{\hbar^2} (E - U) \quad (1.7)$$

Then an electromagnetic wave with frequency ω in a medium with a refractive index of n is analogous to a quantum particle with energy E in a potential U .

Quantum particles are known to ‘tunnel’ through potential barriers [19-21] and there exist situations where electromagnetic ‘tunnelling’ also occurs. One situation in the electromagnetic regime where tunnelling occurs is along a waveguide containing a barrier (a region where propagation does not occur). Such a region is said to be evanescent.

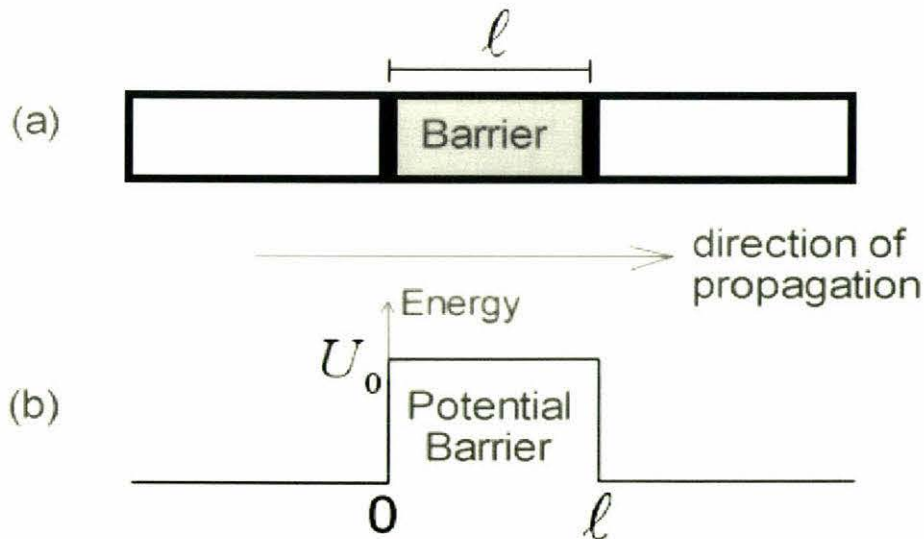


Figure 1.1: Tunnelling analogies. (a) A waveguide with an evanescent barrier of length ℓ . (b) Analogous potential quantum barrier of length ℓ and height U_0 .

In this study, the waveguide with a barrier can be considered in 3 sections. It is required that the dominant waveguide mode be freely propagated through the first and third sections, this implies that the signal frequencies f be greater than f_1 (the lower cut-off frequency in regions 1 and 3). It is also required that the dominant mode be evanescent in the second section, this implies that f be less than f_2 (the upper cut-off frequency in region 2), see equation (2.11) in section 2.2.1

1.3 Tunnelling time and the Hartman effect

How long does a quantum particle or electromagnetic wave take to tunnel through a barrier region? This question has created much interest and speculation over recent years. In 1962, Thomas E. Hartman published a paper [19] giving analytic expressions for the time spent by a quantum particle tunnelling through a potential barrier. He found that the transmission times were less than the time that would be required for the incident particle to travel a distance equal to the barrier length with speed c . This result leads to a finite tunnelling time that is independent of the barrier length. In the case of electromagnetic tunnelling through a barrier within a waveguide, there is a noticeable time delay. This delay arises from phase changes on transmission through the barrier interfaces and not from the traversal of the barrier. Likewise, studies on the dwell times of a quantum particle tunnelling through a quantum potential barrier have shown that the tunnelling particles spend equal amounts of time near the entrance and exit faces of the barrier, but vanishingly little within the barrier [20, 21]. Because of this, superluminal (faster than light) speeds are predicted for both quantum and electromagnetic tunnelling. Theoretical studies based on the 1-D Klein-Gordon equation show that a Gaussian wavepacket incident on the left side of a barrier, emerges on the right side at an earlier time than would appear to be allowed by causal propagation [22]. It will be shown later in this thesis why a Gaussian signal is the preferred signal to use in such an investigation. The superluminal experiments mentioned in section 1.1 are in accordance with the Hartman effect.

1.4 Electromagnetic tunnelling through a waveguide

Throughout the 1990's a group of scientists under the leadership of Günter Nimtz at the University of Cologne carried out 'superluminal' experiments [8-13] using a waveguide with various types of barriers. Their results suggested that for particular barriers, a 'signal' could be sent faster than the speed of light. One of their studies involved the experimental investigation of electromagnetic waveguide tunnelling through both dissipative and non-dissipative barriers [8]. Barrier lengths of 4.9 cm and 6.47 cm were fabricated and the results of this experiment were presented as two graphs, refer to figure 1.2. The first graph showed the modulus of the transmission coefficient as a function of frequency while the second showed the phase shift of the transmission coefficient as a function of frequency. Time domain signals can be constructed from these frequency domain experiments.

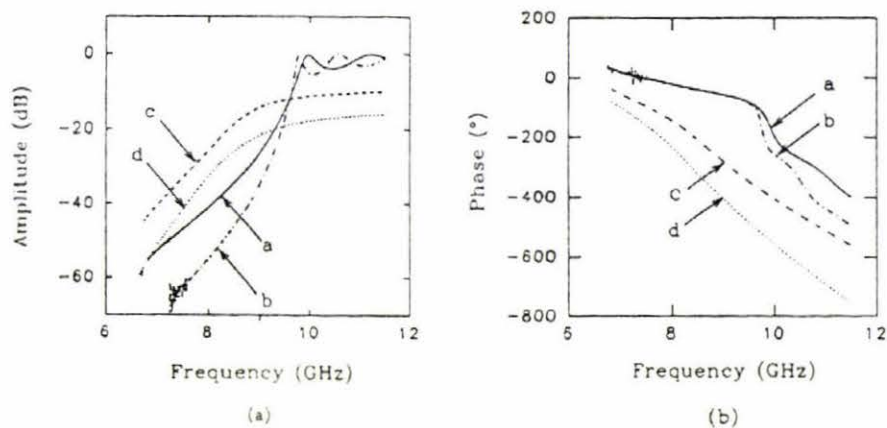


Figure 1.2: Experimental Results. Reproduced from Fig.2, page 1381, Nimtz *et al.* [8]. Transmission coefficient magnitude against frequency (a) and phase against frequency (b) for two barrier lengths a,c=4.9cm and b,d=6.47cm. c and d are filled with a complex dielectric medium.

It was claimed that for the non-dissipative barriers, the traversal time was independent of barrier length resulting in superluminal speeds. The group speeds that were calculated from the phase time for the 7GHz component gave speeds of 1.1c and 1.5c through the 4.9cm and 6.47cm non-dissipative barriers respectively. Their results also showed that with dissipation, the phase shift became dependent on barrier length. The propagation phase change in this case is dominant and the Hartman effect was not observed. Consequently, superluminal speeds were not observed. The group speeds calculated gave speeds of 0.7c for both dissipative barrier lengths (again for the 7GHz component).